

RESEARCH ARTICLE

Newton-GMRES-Method for the Scritinization of electric double layer and surface roughness on EHL line contact problem

V. B. Awati*, P. M. Obannavar, and N. Mahesh Kumar

Department of Mathematics, Rani Channamma University, Belagavi, Karnataka, India-591156

Phone: 0831-2565246

ABSTRACT - The electric double layer phenomenon exists on the solid interface under the water-liquid condition. The water molecules are ionized and adhered in the interface forming the sturn layer is a diffused layer in which molecules can move with the movement of bulk of molecules. Because of these two characteristics, the boundary layer of water molecules is called the electric double layer. The aim of present study is to explore the impact of two fraction surfaces of electric double layer (EDL) on a thin water lubricating film on an elasto-hydrodynamic lubrication (EHL) line contact problem with a sinusoidal surface roughness. The governing modified Reynolds and film thickness equations are based on mathematical model of electro-viscosity of asymmetrical electrical double layer is analyzed numerically. The viscosity-pressure relation of water and theoretical evaluation pertaining to the effect of electric double layer on film-thickness and pressure distribution of EHL with water film of line contact problem is discussed in detail. The effect of zeta potential on film thickness and pressure is determined using Newton's-GMRES method with Daubechies D6 wavelet as a pre-conditioner. The results predict that, EDL has less impact on pressure distribution and significant impact on film thickness. The obtained results are compared with results of Dowson and Higginson which are comparable.

ARTICLE HISTORY

Received : 11th Oct. 2022

Revised : 13th Jan. 2023

Accepted : 01st Mar. 2023

Published : 23rd Mar. 2023

KEYWORDS

Electric double layer

ElastoHydrodynamic

Thin film

Newton-GMRES

Daubechies D6 wavelet

1.0 INTRODUCTION

The interface between solid and liquid there exist a phenomenon known as electric double layer (EDL) and effective range of this phenomenon is about 12nm. It is a surface phenomenon, and their impact is more pronounced when dimension of channel is of the same order of EDL thickness. The existence of EDL in micro-channel is to be retard liquid flow, resulting in to streaming potential [1]. In a thin lubricating film, the rheological properties of lubricant in micro-channel affected by EDL and properties of lubricant are quite different from that of thick lubrication was discussed through experiments [2, 5]. Luo et al. [6] thoroughly analyzed the difference between EHL and thin film lubrication (TFL), further measured the fluid film thickness with different operating conditions for various lubricants and results were compared with the experimental findings. The new technique is to measure the film thickness in nano scale was introduced by Wen and Luo [7] and discussed the characteristics of TFL. Prieve and Bike [8, 9] analyzed the presence of electro-kinetic contributions in hydrodynamic force acting on two-dimensional sliding bodies. Also, extended this work to three-dimensional flows for bodies demeaning the thin double layer in which sliding and squeezing motions are considered.

Zhang and Umehara [10] introduced the hydrodynamic lubrication theory by considering ceramics materials. By using Zhang and Umehara's modified Reynolds equation, Wong et al. [11] numerically discussed the effect of EDL on hydrodynamic lubrication as well as EHL problems. Bai et al. [12-14] proposed a detailed mathematical model to examine the electro-viscous effect due to EDL and conducted several experiments to understand EDL effects on thin film lubrication. There are two types of EDL structures viz., symmetrical and asymmetrical. In the past few decades many researchers have studied the impact of EDL on lubricant properties which are usually considered for the structures of two EDL and are symmetrical [15]. In fact, there are many tribopairs composed of different materials that have different electrical properties, it gives rise to EDL structures which are largely asymmetrical. Zuo et al. [16, 17] presented the asymmetrical EDL effects on thin film of thermal EHL point contact problem and noticed that, the apparent viscosity mainly depends on sum of two zeta potentials. The EDL leads to be remarkable increase in apparent viscosity of lubricant when lubricating film is very thin and pressure is minimal. The effect of electric double layer in the film thickness and pressure distribution of EHL line contact problem lubricated with water film was analyzed by Chen et al. [18]. Clermont et al. [19] numerically discussed the effect of temperature on EDL and concluded that, temperature step provokes the chemical reaction activity and charge redistribution in the liquid volume.

Lubrecht et al. [20] presented the multilevel multi-integration technique to solve elastic deflection integral in the film thickness equation. The EHL elliptical contact problem lubricated with grease was analyzed by Yang and Qiang [21]. Venner [22] introduced multi-grid technique to solve EHL problems, which is one of the most widely used efficient

*CORRESPONDING AUTHOR | V. B. Awati | ✉ awati_vb@yahoo.com

numerical technique. The multilevel solver is extended to EHL elliptical/point contact problems, predict central film thickness and derived the empirical formula. The effect of variations such as load, speed and reduced radii of curvature of surface was discussed in detail by Nijenbanning et al. [23]. Lu et al. [24] analyzed the solution of EHL line contact problem by implementing a higher order discontinuous Galerkin method. The EHL solutions based on new numerical and experimental methods which are more efficient for in-depth study of thermal EHL problems. Starved EHL and roughness with Newtonian and non-Newtonian lubricants with soft, hard bearing components was discussed by Morales –Espejel [25]. Chen and Ford [26, 28] were first to explore the use of wavelet pre-conditioner for the solution of large system of equations, and checked the efficiency of pre-conditioner by implementing it to EHL line contact problem. Awati et al. [29] discussed the solution of EHL point contact problem with bio-based oil as lubricant and noticed that, the minimum film thickness decreases with increase in load; at the same time central film thickness increases with increase in load at constant speed.

Awati and Naik [30] used multigrid method to determine the solution of EHL line contact problem lubricated with grease witnessed that, the decrease in minimum film thickness and pressure spike as the rheological index decreases. Also, the solution of thermal EHL line contact problem were analyzed by Awati et al. [31] and predict that, the reduction in minimum film thickness for high speed. In another problem, Chen et al. [32] analyzed point contact EHL on the surface of particle reinforced composite by considering Ree-Eyring EHL model. Xiao and Shi [33] numerically investigated the stiffness and damping of transient non-Newtonian thermal EHL point contact for crowned herringbone gears. Zhao and Wong [34] discussed thermal EHL analysis of slip/ no-slip contact at high slide-to-roll ratio and concluded that, the combined mechanism of boundary slip and thermal effects on film formation was revealed numerically. Awati and Kumar [35] discussed the piezo-viscous EHL line contact problem by using Newton-GMRES method with Daubechies D6 wavelet as preconditioner.

2.0 KRYLOV SUBSPACE METHODS

Krylov subspace methods (KSM) are generally used to solve sparse linear system of equations.

$$Ax = b, \quad A \in \mathbb{R}^{n \times n}, \quad b \in \mathbb{R}^{n \times 1} \tag{1}$$

Our aim is to determine the accurate solution of Eq. (1) with less number of iterations by constructing stable basis for KSM involving the extension of stable bases with suitable/appropriate orthogonalization. Let us consider x_0 as an initial approximation to the solution of Eq. (1) and is obtained by,

$$r_0 = b - Ax_0 \tag{2}$$

The Krylov subspace is generated by the vectors $r_0, Ar_0, A^2r_0, \dots, A^{m-1}r_0$ of dimension m, generated by A and r_0 that is,

$$K_m(A, r_0) = \text{span}\{r_0, Ar_0, A^2r_0, \dots, A^{m-1}r_0\} = K_m \tag{3}$$

with $K_1 \subset K_2 \subset \dots \subset K_{m-1} \subset K_m$ are the nested spaces and for each step dimension of the spaces is increased by one. In this process dimension cannot cross the value of m, but it will be smaller than the value of m. $K_m(A, r_0)$ is invariant under A if $\exists m \leq n$.

$$K_m(A, r_0) = AK_{m-1}(A, r_0)$$

Let x_k be the approximate solution of Eq. (1) of the form

$$x_k = x_0 + z_k \tag{4}$$

where, x_0 is initial approximation and z_k is element of Krylov subspace $K_m(A, r_0)$. In order to choose this z_k , we make use of the Arnoldi's orthogonalization process. i.e. the first k orthogonal vectors v_j are used such that

$$z_k = \sum_{j=1}^k v_j y_j = [v_1, v_2, \dots, v_k] y = V_k y \tag{5}$$

a with $y \in \mathbb{R}^k$ and $\text{span}\{v_1, v_2, v_3, \dots, v_k\} \in K_m(A, r_0)$. The starting vector of Arnoldi process will be $v_1 = \frac{r_0}{\|r_0\|_2}$, then $H_k = V_k^T A V_k$ is upper $k \times k$ Hessenberg matrix and the entries will be scalars generated by Arnoldi method

$$H_k = \begin{bmatrix} h_{11} & h_{12} & \cdots & h_{1,k-1} & h_{1k} \\ h_{21} & h_{22} & \cdots & h_{2,k-1} & h_{2k} \\ & h_{32} & \cdots & h_{3,k-1} & h_{3k} \\ & & \ddots & \ddots & \vdots \\ & & & h_{k,k-1} & h_{k,k} \end{bmatrix}_{k \times k}, \tag{6}$$

where, $k \leq m \leq n$

The generated k orthogonal vectors v_j satisfy,

$$A_{n \times n}(V_k)_{n \times k} = (V_{k+1})_{n \times (k+1)}(H_{k+1})_{(k+1) \times k} = V_k H_k + h_{k+1,k} v_k + 1e_k^T \tag{7}$$

The relation between vectors v_j and Hessenberg matrix $(\bar{H}_k)_{(k+1) \times k}$ is given by,

$$AV_k = V_k \bar{H}_k \tag{8}$$

Now by using Least square technique, we get,

$$\min_{z \in K_m} \|b - A[x_0 + z]\| = \min_{z \in K_m} \|r_0 - Az\| \tag{9}$$

by substituting $z = V_k y$, the minimized norm becomes,

$$J(y) = \|\beta v_1 - AV_k y\| \tag{10}$$

where, $\beta = \|r_0\|$. Substituting Eq. (8) in Eq. (10), we get,

$$J(y) = \|V_{k+1}[\beta e_1 - \bar{H}_k y]\| \tag{11}$$

where e_1 is the first column of the $(k+1) \times (k+1)$ identity matrix, we also know that V_{k+1} is l_2 -orthonormal and satisfy the condition,

$$J(y) = \|\beta e_1 - \bar{H}_k y\| \tag{12}$$

Eq. (12) represents the projection of large system of equations which is much smaller than Eq. (1). It has unique solution since A is non-singular matrix. Eq. (12) is solved for y , by using QR factorization of \bar{H}_k and Givens rotations.

Finally, the approximate solution is $x_k = x_0 + V_k y_k$.

These methods are applicable when the coefficient matrix A has special properties like symmetry, positive definiteness. The conjugate gradient method (CGM) is applied when A is symmetric matrix and positive definite, the Minimal residual scheme (MINRES) is used when A is an indefinite and symmetric matrix and Generalized minimal residual method (GMRES) is applicable when A is non-symmetric matrix. These methods require more CPU time and needs a large number of iterations in order to get a desirable accuracy of the solutions. The drawback of these methods includes stagnation of iteration, break down etc., the convergence of these methods depends on spectral properties of A (Eigen value distribution).

The above procedure employed for the solution of system of algebraic equations by using KSM [36]. The numerical implementation of GMRES have advantages viz consistency, robustness, proximity property [37] and these properties makes the method becomes reliable. The convergence behaviour of GMRES is studied with the help of field of values, pseudo spectra and convex hull of a matrix [38]. The super linear convergence occurs when A is diagonalizable. For more details about the convergence of GMRES method is found in [39]. GMRES with Householder Gram-Schmidt Orthogonalization and its stability is analyzed in [40].

The main focus of the present study to analyze the The Newton-GMRES method with pre-conditioner technique is employed to analyze the impact of electric double layer on EHL line contact problem. The Pre-conditioning technique is

used to obtain the solution much faster than the usual Newton-GMRES method and it reduce the large condition number of Jacobian matrixes to unity. In the present study, we use Daubechies D6 wavelet as pre-conditioner to determine the solution of EDL and surface roughness on EHL line contact by using Newton-GMRES method. It is illustrated that water can be used as lubricant in machine elements for it is abundantly available in nature, which is environmentally friendly fluid, high thermal conductivity, non-toxicity, cleanliness. Surface roughness are less in ceramic material as compared to other materials. Thus, water as lubricant it cannot be used in steel and iron surface material, but it can be used in the ceramic surface materials.

3.0 GOVERNING EQUATIONS

The mathematical model of EHL line contact problem consist of two rotating balls and cylindrical rollers, in between lubricant flow under an applied load is depicted in the Figure 1. The lubricant flow is described by Reynolds equation and deformation of contacting surfaces (outer ring and cylindrical roller) of roller element bearing is explained by film thickness equation under an applied load.

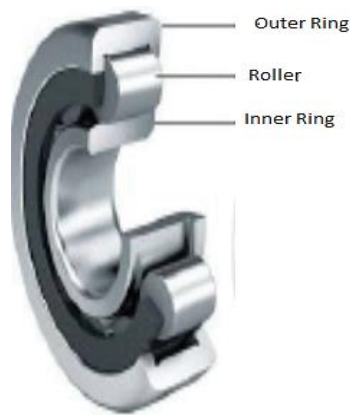


Figure 1. Geometrical interpretation of EHL line contact of roller element bearing

The modified Reynolds equation for electric double layer in line contact EHL problem [10] is given by

$$\frac{d}{dx} \left(\frac{\rho h^3}{12\eta_a} \frac{dp}{dx} \right) = 12u \frac{d(\rho h)}{dx}, \tag{13}$$

where, ρ is the density of lubricant, u is the fixed velocity, η_a is the apparent viscosity, h is the film thickness, p is the pressure of lubricant film and x represents the axis along sliding velocity. The non-dimensional modified Reynolds equation is given by

$$\frac{d}{dX} \left[\varepsilon \frac{dP}{dX} \right] - \frac{d}{dX} (\bar{\rho} H) = 0, \tag{14}$$

where, $\varepsilon = \frac{\bar{\rho} H^3}{\eta_a \lambda}$, $\lambda = \frac{576 R^4 U}{b^*}$, $b = \left(\frac{8WR}{\pi L E'} \right)$ and $L = 1(\text{meter})$.

The modified Reynolds equation which combines with EDL effect is accorded in the viscosity expression. The asymmetrical EDL's apparent viscosity expression is given by Zuo et al. [16].

$$\eta_a = \eta + \frac{3\tilde{\varepsilon}^2 (\xi_1 + \xi_2)^2}{4\pi^2 \kappa^2 h^4 \hat{\lambda}} \left(\frac{\cosh \kappa h - 1}{\sinh \kappa h} - \frac{\kappa h}{2} \right)^2. \tag{15}$$

where, $\tilde{\varepsilon}$ is the absolute dielectric constant of the fluid, η is the lubricant viscosity, κ is the Debye reciprocal length parameter, ξ_1 and ξ_2 respectively denotes zeta potentials of EDL of lower and upper surfaces, $\hat{\lambda}$ is the bulk electrical conductivity. The dimensionless apparent viscosity of asymmetrical EDL is given by,

$$\bar{\eta}_a = \bar{\eta} + (PM) \cdot \frac{1}{H^4} \left[AM - \frac{\kappa H b^2}{2R} \right]^2, \tag{16}$$

where, $PM = \frac{3\bar{\epsilon}^2 (\xi_1 + \xi_2)^2 R^4}{\eta_0 4\pi^2 \kappa^2 b^8 \bar{\lambda}}$, $AM = \frac{\cosh \kappa \left(\frac{Hb^2}{R} \right) - 1}{\sinh \kappa \left(\frac{Hb^2}{R} \right)}$.

The Eq. (16) represents the dimensionless asymmetrical EDL’s apparent viscosity expression, it shows that the EDL exists. The apparent viscosity is directly proportional to square of the sum of two zeta potentials and inversely proportional to the 4th root of film thickness. Therefore, the influence of EDL is significant in very thin film lubrication, but rapidly diminishes when the film thickness increases. The fluid film shape for asymmetrical EDL’s line contact EHL problem along with sinusoidal surface roughness becomes,

$$h(x) = h_0 + \frac{x^2}{2R} - \frac{2}{\pi E'} \int_{x_{in}}^{x_{out}} p(s) \ln(x-s)^2 ds + \mathfrak{R} \tag{17}$$

where, $\mathfrak{R} = \bar{A} \sin \left(\frac{2\pi X_i}{l} \right)$. R denotes the radius of curvature of line contact. The dimensionless parameters used in the present problem are,

$$\begin{aligned} P &= \frac{p}{p_h}, & X &= \frac{x}{b}, & U &= \frac{\eta_0 u}{E'R}, & H &= \frac{hR}{b^2}, & W &= \frac{w}{E'R}, & \bar{\rho} &= \frac{\rho}{\rho_0}, \\ \bar{\eta} &= \frac{\eta}{\eta_0}, & \bar{\eta}_a &= \frac{\eta_a}{\eta_0} & \text{and } S &= \frac{s}{b} \Rightarrow bdS = ds. \end{aligned} \tag{18}$$

The non-dimensional fluid film thickness [41] is given by,

$$H = H_0 + \frac{X^2}{2} - \frac{2}{\pi E'} \int_{X_{in}}^{X_{out}} P(S) \ln(X-S)^2 dS + \mathfrak{R} \tag{19}$$

where, S is an integration variable, X_{in} and X_{out} are the inlet and outlet coordinates along the direction of x -axis, \mathfrak{R} is the sinusoidal surface roughness and H_0 be the central film thickness.

Pressure-viscosity equation: For a high contact pressure the viscosity of lubricant increases in EHL line contact problem. In the present analysis, we use Roelands pressure-viscosity equation [42], given by,

$$\eta = \eta_0 \exp \left\{ (\ln \eta_0 + 9.67) \left[\left(1 + 5.1 \times 10^{-9} p \right)^{0.68} - 1 \right] \right\} \tag{20}$$

The dimensionless form of Roelands pressure-viscosity relation becomes,

$$\bar{\eta} = \exp \left\{ (\ln \eta_0 + 9.67) \left[\left(1 + 5.1 \times 10^{-9} P p_h \right)^{0.68} - 1 \right] \right\} \tag{21}$$

where η_0 is atmospheric viscosity of lubricant and p_h is maximum hertzian pressure.

Density-pressure relation: The lubricant density-pressure relationship for oil and water [43] is given as,

$$\rho = \rho_0 \left(1 + \frac{0.6 \times 10^{-9} p}{1 + 1.7 \times 10^{-9} p} \right). \tag{22}$$

where, ρ_0 is the atmospheric density of lubricant. The non-dimensional form of Eq. (22) becomes,

$$\bar{\rho} = \left(1 + \frac{0.6 \times 10^{-9} P p_h}{1 + 1.7 \times 10^{-9} P p_h} \right). \tag{23}$$

Load balance equation: The load balance equation for EHL line contact problem becomes,

$$\int_{x_{in}}^{x_{out}} p dx = w \tag{24}$$

The dimensionless form of Eq. (24) is given by,

$$\int_{x_{in}}^{x_{out}} P dX = \frac{\pi}{2} \tag{25}$$

The relevant inlet and outlet boundary conditions for the proposed problem becomes,

$$P = 0 \quad \text{at} \quad X = X_{in} \quad \text{and} \quad P = \frac{dP}{dX} \quad \text{at} \quad X = X_{out}. \tag{26}$$

4.0 METHOD OF SOLUTION

4.1 Discretization of Governing Equations

To analyze the impact of electric double layer on EHL line contact problem, the governing equations viz Reynolds, film thickness and load balance are discretized by using second order finite difference approximations in the computational domain $X_{in} = -4$, $X_{out} = 1.4$, and the domain is divided into 512 grid points and critical point X_c is to be determined during the calculation process. The modified Reynolds equation and boundary conditions are discretized as,

$$\frac{\varepsilon_{i-1/2} P_{i-1} - \left(\varepsilon_{i-1/2} + \varepsilon_{i+1/2} \right) P_i + \varepsilon_{i+1/2} P_{i+1}}{\Delta X^2} = \frac{\bar{\rho}_i H_i - \bar{\rho}_{i-1} H_{i-1}}{\Delta X} \tag{27}$$

where, $\Delta X = X_i - X_{i-1}$, $\varepsilon_{i \pm 1/2} = \frac{\varepsilon_i \pm \varepsilon_{i \pm 1}}{2}$, $\varepsilon_i = \frac{\rho_i H_i^3}{\eta a_i \lambda}$

and,

$$P(X_{in}) = 0 \quad \text{and} \quad \frac{P(X_{out}) - P(X_{out-1})}{\Delta X} = 0 \tag{28}$$

The film thickness equation is discretized as,

$$H_i = H_0 + \frac{X_i}{2} - \frac{1}{\pi} \sum_{j=1}^n K_{ij} P_j + \bar{A} \sin \left(\frac{2\pi X_i}{1} \right) \tag{29}$$

where, $K_{ij} = - \left(i - j + \frac{1}{2} \right) \Delta X \left[\ln \left(\left| i - j + \frac{1}{2} \right| \Delta X \right) - 1 \right] + \left(i - j - \frac{1}{2} \right) \Delta X \left[\ln \left(\left| i - j - \frac{1}{2} \right| \Delta X \right) - 1 \right]$

The load balance equation is discretized as,

$$\Delta X \sum_{i=1}^n \frac{(P_i + P_{i+1})}{2} = \frac{\pi}{2} \tag{30}$$

5.0 SOLUTION PROCEDURE

The discretization of Reynolds and film thickness equations results into a non-linear system of algebraic equations and these equations are numerically solved by using Newton's GMRES method along with Daubechies D6 wavelet as a preconditioner. The Newton's method involved Jacobian matrix which comprises a system of linear equations and these equations are solved by GMRES method. In case condition number of Jacobian matrix is large the convergence of iterative method is very slow. To accelerate the convergence of iterative method, we use Daubechies D6 wavelet as a preconditioner which reduces the condition number of Jacobian matrix to unity. Also, the number of non-zero entries are accumulated around the principle diagonal entries, so the solution is obtained much faster than the usual GMRES method. The main advantage of GMRES method is that, it always converges to the required accuracy of the solution which provides the robustness and dependability. The convergence criterion of GMRES method for a linear system of equations $Ax = b$ is given by $\|Ax - b\|_2 \leq Gtol \|b\|_2$ [44].

The study of Ford et al. [45] is evident that, the Newton-GMRES method with preconditioning technique works very well for the system of dense, non-symmetric linear algebraic equations arising from isothermal EHL line contact problem. The authors demonstrated the method by using Discrete Wavelet transform with permutations (DWTPer) preconditioner, compared the results with other preconditioning technique and discussed the convergence of the method. Also, Ford and Chen [46] analyzed the solution of thermal EHL line contact problem with Daubechies D4 and Haar wavelet as a preconditioner. This will enhance the convergence rate of Newton-GMRES method. The procedure for the implementation of Newton-GMRES method and preconditioner is explained in detail [45]. Authors like Bujurke et al. [47] and Awati et al. [35] implemented the method for various EHL problems and the results agree with earlier findings. The obtained pressure values are used to calculate film thickness profiles; simultaneously with multi-level multi-integration (MLMI) method is used to obtain the solution of deformation integral. The load balance equation is verified and h_0 is corrected and again film thickness values are used to obtain new pressure values. This process is repeated until the required accuracy of the pressure is obtained.

6.0 RESULTS AND DISCUSSION

In this work, the problem of EHL line contact with effect of electric double layer (EDL) on film thickness and pressure profiles with sinusoidal roughness is numerically analyzed. The operating parameters are taken from Chen et al. [18] in the present analysis. Further, the friction pairs which are composed of steel (Fe) and sapphire (Al_2O_3) having elastic moduli are 206 and 380 GPa respectively. To make the simplification, we use same Poisson's ratios for both the materials i.e., 0.3. Moreover sliding velocity is taken as 1m/s, 2m/s with maximum hertzian pressure $p_h = 0.5GPa$ and $p_h = 0.3GPa$, with 512 grid points and load $W = 1.8224 \times 10^{-05}$, the absolute value of sum of two zeta potentials are taken as 0mV, 150mV, 300mV throughout the analysis. The numerical investigation of governing problem is analyzed by using Newton-GMRES method with Daubechies D6 wavelet as pre-conditioner. The main aim of this method is to reduce the condition number of Jacobian matrixes which converges much faster otherwise convergence is very slow.

Figure 2, depicts the pressure distribution of EHL line contact problem with absolute value for sum of two zeta potentials 0mV, 150mV, 300mV. In particular $|\xi_1 + \xi_2| = 0$ the EDL effect of EHL line contact problem reduces to a normal isothermal EHL line contact problem, whereas $|\xi_1 + \xi_2| = 150mV$, $|\xi_1 + \xi_2| = 300mV$, shows the effect of EDL on EHL line contact problem with constant load $W = 1.8224 \times 10^{-05}$ and speed $U = 1.7301 \times 10^{-13}$. It is noticed that, there is no change in pressure profiles it means that, the effect of EDL on pressure is minimal. The results agree with the earlier findings of Wong et al. [11], Zuo et al. [16] and Chen et al. [18].

Figure 3, illustrates the film thickness profiles of EHL line contact problem for constant load and speed viz. $W = 1.8224 \times 10^{-05}$ $U = 1.7301 \times 10^{-13}$ with varying absolute value of sum of two zeta potentials. It is observed that, the film thickness increases with increase in the absolute value of sum of two zeta potentials i.e. $|\xi_1 + \xi_2| = 0mV, 150mV, 300mV$ and larger value of sum of two zeta potentials leads to thicker fluid film thickness. This shows the effect of EDL on film thickness is more pronounced as compare to pressure profiles. The earlier findings [11, 16, 18] also illustrates the same behaviour.

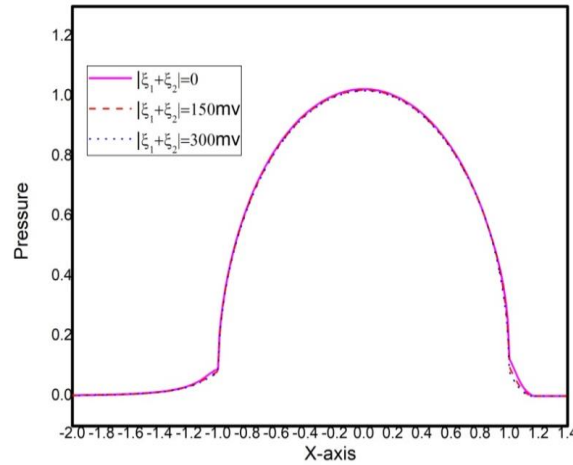


Figure 2. Pressure profiles of EDL with varying zeta potentials 0mV, 150mV,300mV at constant load $W = 1.8224 \times 10^{-05}$ and speed $U = 1.7301 \times 10^{-13}$

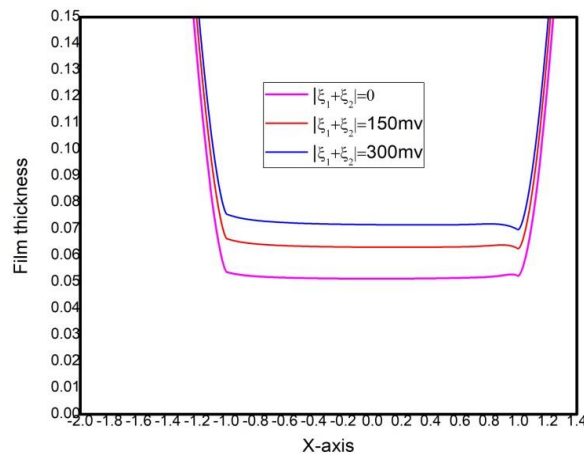


Figure 3. Film thickness profiles of EDL with varying zeta potentials 0mV, 150mV, 300mV at constant load $W=1.8224 \times 10^{-05}$ and speed $U=1.7301 \times 10^{-13}$

Further, consider the sinusoidal surface roughness on film thickness equation, pressure and film thickness profiles are illustrated in Figure 4, and Figure 5, for a constant load $W = 1.8224 \times 10^{-05}$ and speed $U = 1.7301 \times 10^{-13}$ with varying sum of two zeta potentials. It depicts that, after certain amplitude value it ruptures the fluid film, the range of amplitude is 0.05m to 0.115m for domain having 512 grid points. The nature of pressure and film thickness profiles are same as that of [31].

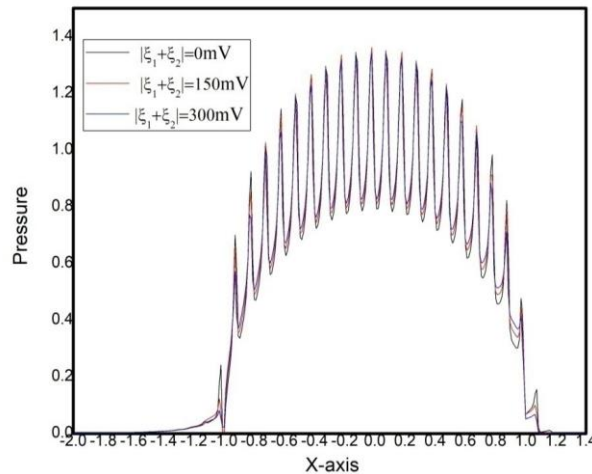


Figure 4. Pressure profiles with roughness by varying zeta potentials 0mV, 150mV, 300mV at constant load $W=1.8224 \times 10^{-05}$ and speed $U=1.7301 \times 10^{-13}$

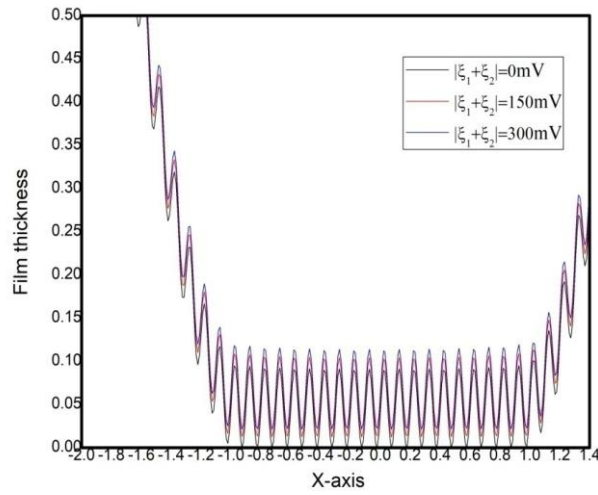


Figure 5. Film thickness profiles with roughness by varying zeta potentials $0mV$, $150mV$, $300mV$ at constant load $W=1.8224 \times 10^{-05}$ and speed $U=1.7301 \times 10^{-13}$

For a constant speed $U = 1.7031 \times 10^{-13}$ and $|\xi_1 + \xi_2| = 300mV$, with varying load $W = 1.3522 \times 10^{-05}$ to 3×10^{-05} was depicted in Figure 6, and Figure 7. In Figure 6, pressure profiles are same for all loads, whereas film thickness profiles in Figure 7, decreases as load increases.

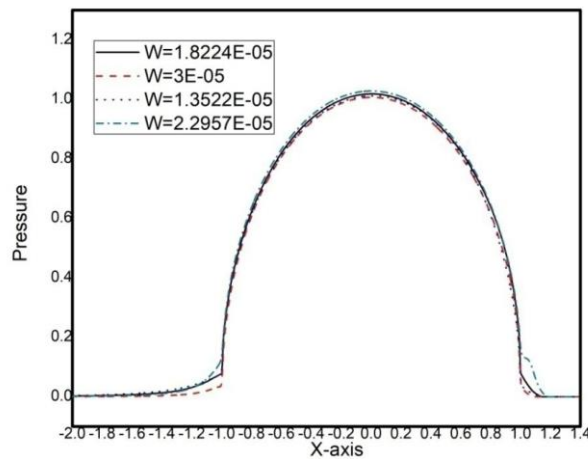


Figure 6. Pressure profiles with load varying from $W=1.3522 \times 10^{-05}$ – 3×10^{-05} at a constant speed $U=1.7301 \times 10^{-13}$ and zeta potential $300mV$

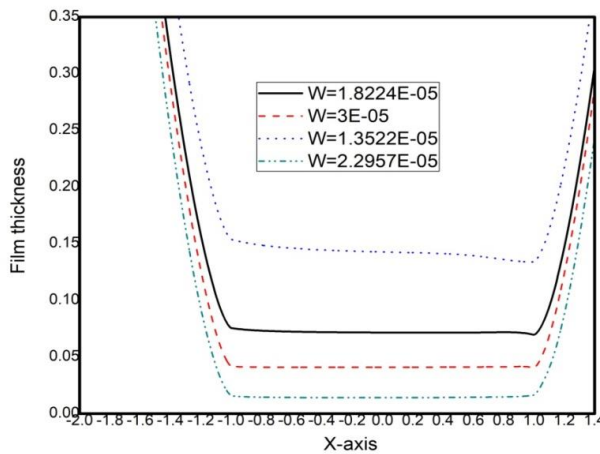


Figure 7. Film thickness profiles with load varying from $W = 1.3522 \times 10^{-05}$ – 3×10^{-05} at a constant speed $U=1.7301 \times 10^{-13}$ and zeta potential $300mV$

The maximum hertzian pressure is 0.3GPa, Figure 8 and Figure 9 demonstrates the pressure and film thickness profiles for a constant load $W = 6.5605 \times 10^{-05}$ and speed $U = 3.4061 \times 10^{-13}$ with varying sum of two zeta potentials from 0 to 300mV . It predicts that, the EDL effect on pressure profiles is minimum and effect of EDL on film thickness was noticeable as compare to pressure distributions, also minimum film thickness values are greater than that of minimum film thickness for $W = 1.8224 \times 10^{-05}$, $U = 1.7031 \times 10^{-13}$.

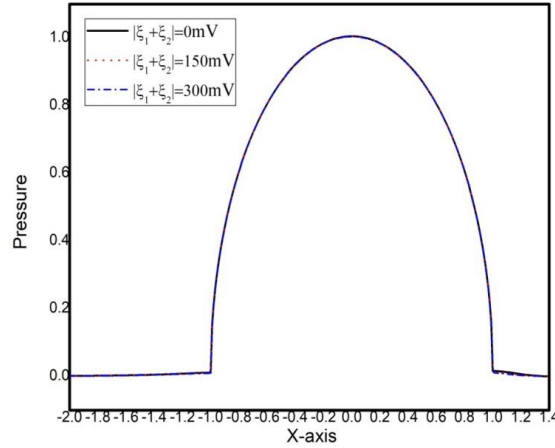


Figure 8. Pressure distribution with maximum pressure 0.3GPa at a constant load and speed $W= 6.5605 \times 10^{-05}$, $U=3.4061 \times 10^{-13}$ with varying zeta potentials 0mV, 150mV, 300mV

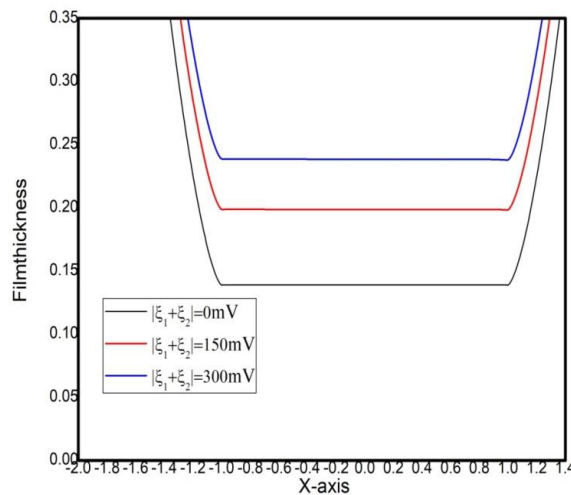


Figure 9. Film thickness distribution with maximum pressure 0.3GPa at a constant load and speed $W= 6.5605 \times 10^{-05}$, $U=3.4061 \times 10^{-13}$ with varying zeta potentials 0mV, 150mV, 300mV

Figure 10, and Figure 11, illustrates, the pressure and film thickness profiles for constant load $W = 1.8224 \times 10^{-05}$ and $|\xi_1 + \xi_2| = 300\text{mV}$ with varying speed $U = 1.7031 \times 10^{-13}$ to 1×10^{-12} . It shows that, pressure profiles are indistinguishable, and film thickness profiles increases with increase in speed. Figures 6 to 11, shows the same characteristics as predicted in Dowson and Higginson [43] for various values of load, speed and material properties. The effect of EDL is more pronounced in the case of film thickness profiles, these are visualised and compared with earlier findings of Wong et al. [11], Zuo et al. [16], Chen et al. [18].

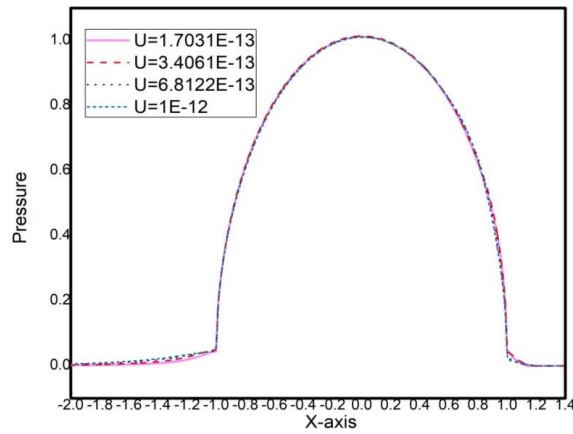


Figure 10. Pressure profiles with speed varying $U = 1.7301 \times 10^{-13}$ to 1×10^{-12} at constant load $= 1.8224 \times 10^{-05}$ and zeta potential $300mV$

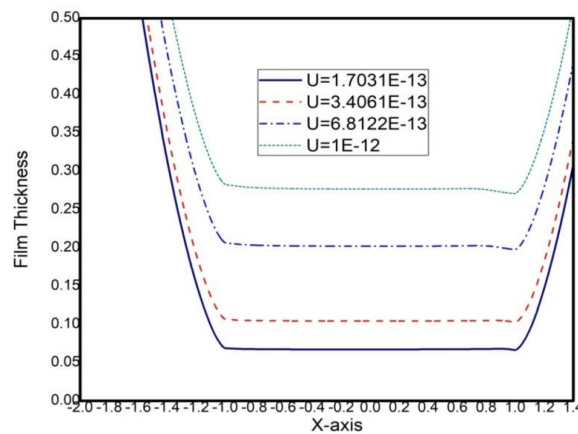


Figure 11. Film thickness distribution with speed varying $U = 1.7301 \times 10^{-13}$ to 1×10^{-12} at constant load $W = 1.8224 \times 10^{-05}$ and zeta potential $300mV$

Table 1 shows the comparison of minimum and central film thickness values for $W = 1.8224 \times 10^{-05}$, $U = 1.7031 \times 10^{-13}$ and $|\xi_1 + \xi_2| = 0mV$ with the Dowson and Higginson [48] empirical values. By considering water as lubricant a very thin film of size less than 100nm is noticed and it is known as thin film lubrication. The film thickness values are too small as compared to Dowson and Higginson [48] and these values are valid for Newtonian fluid.

Table 1. The minimum and Central film thickness values are compared with Dowson and Higginson [48] empirical values

LoadW	Speed U	Central film thickness	Minimum film thickness	Hmin Dowson	Hcen Dowson
1.8224E-05	1.7031E-13	2.1069E-08	2.1208E-08	1.2551E-06	1.3325E-05
3E-05	1.7031E-13	4.4843E-08	4.377E-08	1.1763E-06	1.2735E-06
1.8224E-05	3.4061E-13	4.8403E-08	4.766E-08	2.0389E-06	2.2060E-06
1.8224E-05	6.8122E-13	1.1541E-07	1.13E-07	3.3121E-06	3.6520E-06

7.0 CONCLUSION

The governing equations are used to discuss the impact of electric double layer on EHL line contact problem lubricated with water. The following conclusions are drawn from the above study.

- 1) Water is used as lubricant in machine elements for its abundant availability in nature, environmentally friendly fluid, high thermal conductivity, non-toxicity and cleanliness.
- 2) The effect of absolute value of sum of two zeta potentials on pressure distribution is minimal.

- 3) The film thickness increases with the increase in absolute value of sum of two zeta potentials.
- 4) The film thickness for $0.3GPa$ with speed $U = 3.4061 \times 10^{-13}$ is thicker than that of $0.5GPa$ with speed $U = 1.7301 \times 10^{-13}$.

Pressure and film thickness profiles exhibit the typical EHL profiles under sinusoidal roughness and it ruptures the film thickness after certain amplitude i.e., 0.115m.

8.0 REFERENCES

- [1] W.-L. Li, "Effects of electrodouble layer (EDL) and surface roughness on lubrication theory," *Tribology Letters*, vol. 20, pp. 53-61, 2005.
- [2] C. Terzaghi, "The static rigidity of plastic clays," *Journal of Rheology*, vol. 2, no. 3, pp. 253-262, 1931.
- [3] L. Ren, D. Li, and W. Qu, "Electro-viscous effects on liquid flow in microchannels," *Journal of Colloid and Interface Science*, vol. 233, no. 1, pp. 12-22, 2001.
- [4] L. Ren, W. Qu, and D. Li, "Interfacial electrokinetic effects on liquid flow in microchannels," *International Journal of Heat and Mass Transfer*, vol. 44, no. 16, pp. 3125-3134, 2001.
- [5] D. Li, "Electro-viscous effects on pressure-driven liquid flow in microchannels," *Colloids and Surfaces A: Physicochemical and Engineering Aspects*, vol. 195, no. 1-3, pp. 35-57, 2001.
- [6] J. Luo, S. Wen, and P. Huang, "Thin film lubrication. Part I. Study on the transition between EHL and thin film lubrication using a relative optical interference intensity technique," *Wear*, vol. 194, no. 1-2, pp. 107-115, 1996.
- [7] S. Wen and J. Luo, "Study on thin film lubrication in the nano scale," *Journal-Tsinghua University*, vol. 41, no. 4/5, pp. 63-68, 2001.
- [8] D. C. Prieve and S. G. Bie, "Electrokinetic repulsion between two charged bodies undergoing sliding motion," *Chemical Engineering Communications*, vol. 55, no. 1-6, pp. 149-164, 1987.
- [9] S. G. Bie and D. C. Prieve, "Electrohydrodynamic lubrication with thin double layers," *Journal of Colloid and Interface Science*, vol. 136, no. 1, pp. 95-112, 1990.
- [10] B. Zhang and N. Umehara, "Hydrodynamic lubrication theory considering electric double layer for very thin water film lubrication of ceramics," *JSME International Journal Series C Mechanical Systems, Machine Elements and Manufacturing*, vol. 41, no. 2, pp. 285-290, 1998.
- [11] P. L. Wong, P. Huang, and Y. Meng, "The effect of the electric double layer on a very thin water lubricating film," *Tribology Letters*, vol. 14, pp. 197-203, 2003.
- [12] S. Bai, P. Huang, Y. Meng, and S. Wen, "Modeling and analysis of interfacial electro-kinetic effects on thin film lubrication," *Tribology International*, vol. 39, no. 11, pp. 1405-1412, 2006.
- [13] B. Shaoxian and H. Ping, "Experimental and numerical study on influence of electro-viscosity of electric double layer in thin film lubrication," *Chinese Journal of Mechanical Engineering*, vol. 40, no. 5, pp. 34-38, 2004.
- [14] X.-J. Wang, S.-X. Bai, and P. Huang, "Theoretical analysis and experimental study on the influence of electric double layer on thin film lubrication," *Frontiers of Mechanical Engineering in China*, vol. 1, pp. 370-373, 2006.
- [15] S. Z. Wen, P. Huang, "Interface Science and Technology," *Beijing: Tsing Hua University press*, 2011, pp. 403-11.
- [16] Q. Zuo, P. Huang, and F. Su, "Theory analysis of asymmetrical electric double layer effects on thin film lubrication," *Tribology International*, vol. 49, pp. 67-74, 2012.
- [17] Q. Zuo, T. Lai, and P. Huang, "The effect of the electric double layer on very thin thermal elastohydrodynamic lubricating film," *Tribology Letters*, vol. 45, pp. 455-463, 2012.
- [18] Y. Chen, Q. Zuo, and P. Huang, "Influence of electric double layers on elastohydrodynamic lubricating water film in line contact," *Proceedings of the Institution of Mechanical Engineers, Part N: Journal of Nanoengineering and Nanosystems*, vol. 227, no. 4, pp. 196-198, 2013.
- [19] P. D. S. Clermont, T. Paillat, and P. Leblanc, "Numerical study on the impact of a temperature step on the electrical double layer," *Journal of Electrostatics*, vol. 95, pp. 13-23, 2018.
- [20] A. A. Lubrecht, W. E. Ten Napel, and R. Bosma, "Multigrid, an alternative method of solution for two-dimensional elastohydrodynamically lubricated point contact calculations," *Journal of Tribology*, vol. 109, no. 3, pp. 437-443, 1987.
- [21] Z. Yang, "A study of grease film thickness in elastohydrodynamic rolling point contacts," in *I. Mech. E. Conference Publication*, vol. 1, pp. 97, 1987.
- [22] C. Venner, "Multilevel solution of the EHL line and point contact problems," *Ph.D Thesis*, University of Twente, Netherland, 1991.

- [23] G. Nijenhuis, C. H. Venner, and H. Moes, "Film thickness in elastohydrodynamically lubricated elliptic contacts," *Wear*, vol. 176, no. 2, pp. 217-229, 1994.
- [24] H. Lu, M. Berzins, C. E. Goodyer, and P. Jimack, "High order discontinuous Galerkin method for EHL line contact problems," *Communications in Numerical Methods in Engineering*, vol. 21, no. 11, pp. 643 - 650, 2005.
- [25] P. M. Lugt and G. E. Morales-Espejel, "A review of elasto-hydrodynamic lubrication theory," *Tribology Transactions*, vol. 54, no. 3, pp. 470-496, 2011.
- [26] J. M. Ford, "Wavelet-based preconditioning of dense linear systems," *Ph.D. Thesis*, University of Liverpool, Liverpool, UK, 2001.
- [27] K. Chen, "Matrix preconditioning techniques and applications," *Cambridge University Press*, 2005.
- [28] J. Ford and K. Chen, "Wavelet-based preconditioners for dense matrices with non-smooth local features," *BIT Numerical Mathematics*, vol. 41, pp. 282-307, 2001.
- [29] V. B. Awati and S. Naik, "Multigrid method for the solution of EHL point contact with bio-based oil as lubricants for smooth and rough asperity," *Industrial Lubrication and Tribology*, vol. 70, no. 4, pp. 599-611, 2018.
- [30] B. V. Awati and S. Naik, "A multigrid method for EHL line contact problem with Grease as lubricant," *Mathematical Models in Engineering*, vol. 3, no. 2, pp. 126-134, 2017.
- [31] V. B. Awati, M. Kumar N, and N. M. Bujurke, "Numerical solution of thermal EHL line contact with bio-based oil as lubricant," *Australian Journal of Mechanical Engineering*, vol. 20, no. 1, pp. 231-244, 2022.
- [32] K. Chen, L. Zeng, Z. Wu, and F. Zheng, "Elastohydrodynamic lubrication in point contact on the surfaces of particle-reinforced composite," *AIP Advances*, vol. 8, no. 4, p. 045213, 2018.
- [33] Z. Xiao and X. Shi, "Investigation on stiffness and damping of transient non-newtonian thermal elastohydrodynamic point contact for crowned herringbone gears," *Tribology International*, vol. 137, pp. 102-112, 2019.
- [34] Y. Zhao and P. L. Wong, "Thermal-EHL analysis of slip/no-slip contact at high slide-to-roll ratio," *Tribology International*, vol. 153, p. 106617, 2021.
- [35] V. B. Awati, M. Kumar, "Newton-GMRES method for the solution of piezo-viscous line contact problem with Daubechies wavelet as a preconditioner," *Journal of Modern Industry and Manufacturing*, vol. 1, pp. 1-4, 2022.
- [36] G. Meurant, J. D. Tebbens, "Krylov methods for non-symmetric linear systems: From theory to computations," *Springer*, 2020.
- [37] G. M. D. Carso, O. Menchi and F. Romani, "Krylov subspace methods for solving linear systems," *Technical Report, University of Pisa*, pp. 1-28, 2015.
- [38] N. M. Nachtigal, S. C. Reddy, and L. N. Trefethen, "How fast are nonsymmetric matrix iterations?," *SIAM Journal on Matrix Analysis and Applications*, vol. 13, no. 3, pp. 778-795, 1992.
- [39] A. Greenbaum, "Iterative methods for solving linear systems," *Society for Industrial and Applied Mathematics (SIAM)*, USA 1997.
- [40] J. Drkošová, A. Greenbaum, M. Rozložník, and Z. Strakoš, "Numerical stability of GMRES," *BIT Numerical Mathematics*, vol. 35, no. 3, pp. 309-330, 1995.
- [41] L. G. Houper and B. J. Hamrock, "Fast approach for calculating film thicknesses and pressures in elastohydrodynamically lubricated contacts at high loads," *Journal of Tribology*, vol. 108, pp. 411-420, 1986.
- [42] C. J. A. Roelands, W. O. Winer, and W. A. Wright, "Correlational aspects of the viscosity-temperature-pressure relationship of lubricating oils," *Journal of Lubrication Technology*, vol. 93, no. 1, pp. 209-210, 1971.
- [43] D. Dowson and G. R. Higginson, "Elasto-hydrodynamic lubrication," *Pergamon Press*, Oxford, 1977.
- [44] M. J. Zahr and P.-O. Persson, "Performance tuning of Newton-GMRES methods for discontinuous Galerkin discretizations of the Navier-Stokes equations," in *21st AIAA Computational Fluid Dynamics Conference*, San Diego, June 24 - 27, 2013.
- [45] J. Ford, K. Chen, and L. Scales, "A new wavelet transform preconditioner for iterative solution of elastohydrodynamic lubrication problems," *International Journal of Computer Mathematics*, vol. 75, no. 4, pp. 497-513, 2000.
- [46] J. M. Ford and K. Chen, "Speeding up the solution of thermal EHL problems," *International Journal for Numerical Methods in Engineering*, vol. 53, no. 10, pp. 2305-2310, 2002.
- [47] N. M. Bujurke and M. H. Kantli, "Numerical simulation of influence of surface features on the elastohydrodynamic lubrication of sliding line contact using Krylov subspace method," *Computational Mathematics and Modeling*, vol. 32, no. 2, pp. 198-220, 2021.
- [48] D. Dowson and G. R. Higginson, "The effect of material properties on the lubrication of elastic rollers," *Journal of Mechanical Engineering Science*, vol. 2, no. 3, pp. 188-194, 1960.